NEW LROC WAC TiO_2 ABUNDANCE MAP OF THE MOON. H. Sato[1], M. S. Robinson[1], B. Hapke[2], and S. J. Lawrence[1], [1]Arizona State University, AZ. (hsato@ser.asu.edu), [2]University of Pittsburgh, PA.

Introduction: The global distribution of TiO_2 in the lunar regolith was estimated using Lunar Reconnaissance Orbiter (LRO) Wide Angle Camera (WAC) multi-spectral observations (7 bands from 321 to 689 nm [1]). The spectral slope from UV to visible wavelengths is known to be significantly affected by variations in ilmenite ($FeTiO_2$) abundance [2,3]. Thus we used the WAC 321 and 415 nm bands to estimate TiO_2 abundance. The new TiO_2 abundance map was compared with TiO_2 maps based on the Clementine and Lunar Prospector (LP) data sets.

Methodology: We assumed that the dominant control of the 321 nm over 415 nm band ratio for the mare is ilmenite abundance variation [2,3]. The ratio value was compared to lab analyses of returned lunar soils to establish a conversion from ratio to TiO_2 abundance.

The WAC 321/415 ratio values were derived from ~36 months of observations at each sample-return site. The original pixel scale (average within a frame) of the WAC during the LRO's quasi-circular 50 km orbit period was 423 m for the UV and 83 m for visible bands [4]. In the current elliptical orbit, the pixel scale ranges from 550 to 1170 m/pixel in UV and from 107 to 228 m/pixel in visible bands within the latitudes of sample-return sites (-9° to 26°N). For each site, about 30 UV and 230 visible (per band) observations (image pixels), whose pixel edges are inside a 800 by 800 meter box centered at the exact sample-return spot, were selected from non map-projected WAC images for each band. The DN value of each pixel was converted to the radiance factor (***I/F***) [5], then photometrically normalized by a Hapke function [5] using spatially resolved Hapke parameter maps [1]. To minimize the influence of local features with anomalous albedo (very high or low relative to the sample site), all the pixels that included such local features were removed (determined from ~2 m/pixel Narrow Angle Camera images). The modal value and the standard deviation of the normalized ***I/F*** (***nI/F***) from the down-selected WAC pixels were derived for each band at each sample-return site.

For the lunar sample TiO_2 values, we used the compositional data reported by [6,7]. Several sample-return sites are found at geologically complicated locations, such as the Apollo 17 LRV2 and LRV3 sites, where the Light Mantle partially covers the surface (within ~200 m radius, the average WAC pixel size in UV). These sites are difficult to obtain WAC ratio values that accurately represent the reflectance of the sampled material, and were thus excluded.

A linear correlation was assumed between the TiO_2 contents of the lunar samples and the WAC ratio values [2]. The linear-fit line was obtained by least-square fitting, then a near-global TiO_2 abundance map was created using the fitted line and the 321/415 nm WAC near-global ratio map (70°S to 70°N and 0°E to 360°E, 64 pixel/degree).

The new WAC TiO_2 abundance map (hereafter called $WACTiO_2$) was then compared with the Clementine UVVIS based TiO_2 map [8] (hereafter called $CLMTiO_2$) and the LP Neutron Spectrometer version [9] (hereafter called $LPNTiO_2$). The $WACTiO_2$ and $CLMTiO_2$ were compared in 32 pixel/degrees (947.6 m/pixel at the equator) to minimize scatter due to georeferencing and photometric normalization uncertainties [10] in the Clementine mosaic. The $LPNTiO_2$ was sampled at 2 pixels per degrees, thus the $WACTiO_2$ was down sampled for the comparison.

Results and Discussion: The lunar sample TiO_2 values and the 321/415 nm ratios of the WAC normalized ***I/F*** (***nI/F***) show a strong positive correlation (Fig.1, black dashed line is y = 86.2x - 59.5, R^2 = 0.95). The error bar (standard deviation) is based on all the selected WAC observations (non map-projected pixels) thus includes geologic variation within the 800 m box and ***nI/F*** derivation uncertainties. The sample from Luna 16 was excluded from the fit.

The derived $WACTiO_2$ has negative values within most of the highlands (-0.7 wt% in median, Fig. 2), suggesting very low ilmenite content. Median and standard deviation in each major mare are shown in Table 1. Compared to the $CLMTiO_2$ (Fig. 4), the $WACTiO_2$ shows systematically lower TiO_2 content (2.0 and 1.1

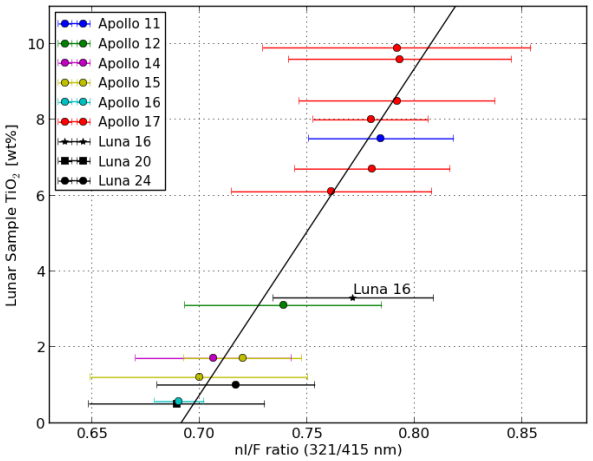

Figure 1. Plot of the TiO_2 content of lunar soils vs WAC ***nI/F*** ratio (321/415 nm) for each mission.

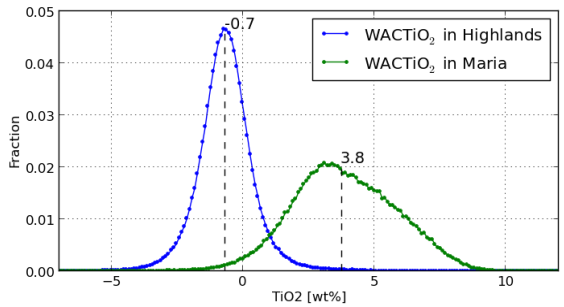

Figure 2. Histogram of $WACTiO_2$. Dashed line and float-number indicate median value of each geologic region.

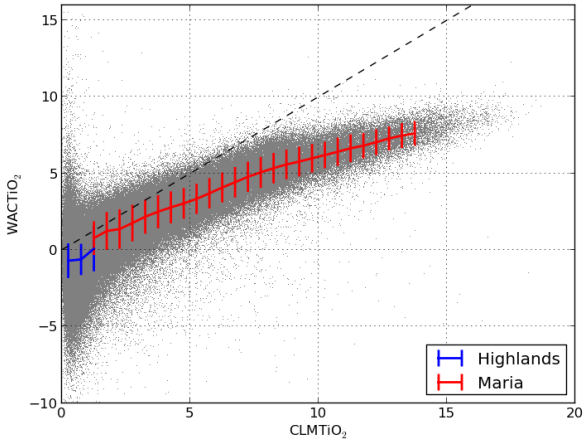

Figure 3. Plot of $CLMTiO_2$ vs $WACTiO_2$. The median and standard deviation in each bin (0.5 wt%) are displayed for the maria (red) and the highlands (blue).

wt% below $CLMTiO_2$ in the maria and in the highland respectively), particularly in high-TiO_2 content maria (e.g. Mare Tranquillitatis -3.1 wt%; Fecunditatis -2.1 wt%; and Oceanus Precellarum -1.8 wt%; see Fig. 4). In some areas (< 0.15% of whole map area) the WAC 321/415 ratios are higher than the highest value of the lunar sample-return sites (0.79, ~8.6 wt%). For those areas TiO_2 values were extrapolated from the linear fit line. Thus the highest $WACTiO_2$ values should be interpreted with extra caution. Other studies have proposed that the $CLMTiO_2$ technique overestimates TiO_2 abundance in areas of high concentrations (e.g. $LPNTiO_2$ [11], Chang'E1 IIM [13], and HST [2]), consistent with the new $WACTiO_2$ values.

The median value of $LPNTiO_2$ - $WACTiO_2$ in the mare is -1.1 wt%. The difference map (2 pixel/degree; Fig. 5) represents that the $WACTiO_2$ is higher (blue area) in the most areas of maria but lower (deep red area) at Copernican crater ejecta blankets (Aristarchus, Copernicus, and Kepler) relative to $LPNTiO_2$. Since each observation of the neutron spectrometer is based on a large field-of-view (about 700 km in diameter [11]), each pixel value of $LPNTiO_2$ accumulates signal from a broader area, which results in fuzzy geologic boundaries. Also the effective depth of the neutron

Table 1. $WACTiO_2$ values in each Mare. [wt%]

Mare	Median	Std.dev.
Tranqillitatis	5.5	2.3
Procellarum	3.5	2.4
Humorum	3.0	1.9
Cognitum	2.9	1.8
Serenitatis	2.7	1.5
Imbrium	2.6	2.1
Nubium	2.5	1.6
Crisium	1.8	1.5
Fecunditatis	1.4	1.8

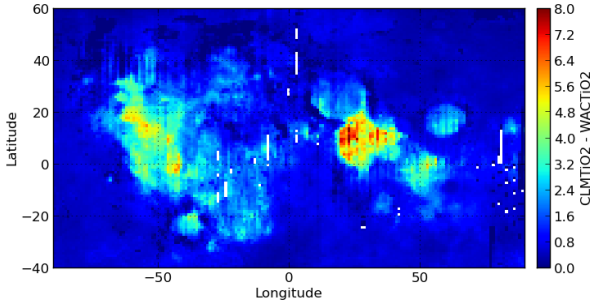

Figure 4. Difference map of $CLMTiO_2$ - $WACTiO_2$. The negative values in $WACTiO_2$ were set to zero before subtraction.

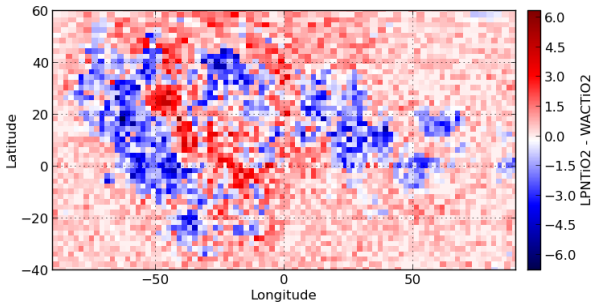

Figure 5. Difference map of $LPNTiO_2$ - $WACTiO_2$ (2 pixel/deg). The negative values in $WACTiO_2$ were set to zero before subtraction.

spectrometer is deeper (~30 cm [12]) than the UV/visible reflectance (several micron [5]). The sharpness and the sampling depth of the two instruments likely influenced the differences between the $WACTiO_2$ and the $LPNTiO_2$ as seen in Fig.5.

References: [1] Sato et al. (2014) *JGR*, v119, doi:10.1002/2013JE004580. [2] Robinson et al. (2007) *GRL*, v34, 15-18. [3] Cloutis et al. (2008) *Icarus*, v197, 321-347. [4] Robinson et al. (2010) *SSR*, v150, p81-124. [5] Hapke (2012) *Theory of Reflectance and Emittance Spectroscopy*, Cambridge Univ. Press, NY. [6] Blewett et al. (1997) *JGR*, v102, E7, p16321-16325. [7] Jolliff (1999) *JGR*, v104, E6, p14123-14148. [8] Lucey et al. (2000) *JGR*, v105, E8, p20297-20305. [9] Elphic et al. (2002) *JGR*, v107, E4, 5024. [10] Barnett and Speyerer (2011) Lunar Science Forum, B-15. [11] Elphic et al. (1998) *Science*, v281, 5382, p1493-1496. [12] Lawrence, et al. (2002) JGR, v107, 5130. [13] Wu et al. (2012) *JGR*, v117, E02001.